Digest Journal of Nanomaterials and Biostructures Vol. 6, No 2, April - June 2011, p. 549 - 556

ENHANCING ANTIBACTERIAL EFFECT OF MULTIWALLED CARBON NANOTUBES USING SILVER NANOPARTICLES

M. PRODANA, D. IONITA, C. UNGUREANU, D. BOJIN, I. DEMETRESCU*
"Politehnica" University of Bucharest, Bucharest, Romania

Taking into account that the increase of specific area as nanosizing effect of carbon nanotubes is connected ussualy with chemical reactivity and toxicity for various soluble and stimulative materials, the present research proposes a method to enhance antibacterial effect using silver nanoparticle. In fact the manuscript is a comparison between antibacterial effect of carbon nanotubes (multiwalled) functionalized and nonfunctionalised in the presence of silver nanoparticles. The nanotubes functionalization is performed according a chemical procedure introducing -COOH groups. Surface analysis type transmission electron microscopy (TEM) and infrared spectroscopy (FTIR) presents topographical aspects of nanotubes. The paper signals new trends in explaining antibacterial effect of silver nanoparticles against growth of *Escherichia coli* bacteria, proposing a model of silver nanoparticles at interface carbon nanotubes/Ag^+ nanoparticles. It is a type Troian Horse model according our data and literature data. The application of such research is related not only to enhance antibacterial effect of materials at nanolevel, but taking into account that carbon nanotubes as other nanomaterials have bilateral nature with two possibilities of high functions and risks the paper contributes to the proper understanding of nanosinzing effect.

(Received March 1, 2011; accepted March 9, 2011)

Keywords: Antibacterial, Carbon nanotubes, Silver nanoparticles, Functionalization

1. Introduction

Carbon nanotubes (CNTs) are allotropes of carbon, members of the fullerene structural family with a cylindrical nanoarchitecture, constructed with length-to-diameter ratio of up to 132 000 000:1 [1]. Having remarkable strength and biocompatibility carbon nanotubes [2] are used in various application depending of their elaboration [3,4] and characterization [5]. Nanotubes are clasified as single-walled nanotubes (SWNTs) and multi-walled nanotubes (MWNTs) and both categories could be functionalized and nonfunctionalized in order to get more adherence for different substrate. In the last decade carbon nanotubes, especially MWNTs were used as components in various composite with biomimetic characteristics [6,7].

Regarding the biocompatibility of multi-walled carbon nanotubes (MWNTs), the viability of fibroblasts, osteoblasts and osteocalcin concentrations in osteoblasts cultures in the presence of nanotubes has been examined, and the results indicated a high level of cell viability and a slight increase of collagen formation. The collagen synthesis induced on nanotubes by cell was supposed to be promising for bioengineering applications of nanotubes as substrates for tissues regeneration. In fact an increase of biocompatibility quantified in a better cell response is expected on various kind of nanoarchitecture type nanotubes due to the increase of the surface available for cell culture, adherence and proliferation [8,9]. Despite this benefit aspect of behaviour some toxicity [10] of carbon nanotubes was observed and such determinations have been one of the challenge questions in nanotechnology [11].

Taking into account that nanotubes are heterogenous materials and their dimensions, functionalization surface charge, and agglomeration have impact on reactivity we have to

*Corresponding author: I_demetrescu@chim.upb.ro

understand that is possible that in specific conditions nanotubes can cross membrane barriers inducing harmful effect such as inflammatory and fibrotic reactions [12]. There are studies showing that CNTs can enter human cells and accumulate in the cytoplasm, causing cell death [13].

However the detection of CNTs harmfull effect became important despite the fact that unfortunately, such research has only just begun and results are still incomplete. Starting from this idea introducing nanoparticles as silver well known antibacterial [14] material become efficiently and leads to propose a model of silver nanoparticles at interface carbon nanonotubes/Ag^+ nanoparticles.

2. Experimental

Regarding silver nanoparticles there are several elaboration methods including biogenic production [14,15].

Our method involves 100 mL of aqueous solution of silver nitrate with a concentration of 0.25 M, and 85mL 0.25 M trisodium citrate. While stirring vigorously, 0.6 mL of 10 mM $NaBH_4$ was added to the solution. Following this the silver nanoparticles were deposited onto carbon nanotubes [16].

The aim of this study is to obtain a good antibacterial effect for multi-walled carbon nanotubes (MWCNTs) by functionalization with Ag nanoparticles [17]. Nanosized particles are investigated using TEM analysys (transmission electrone mycroscopy) with a EM-410 Philips, 60kV mycroscope.

MWCNTs of curled shape have about 20-40 nm in diameter and 0.1-10 µm length are provided by Sigma Aldrich with a purity of 90%.

2.1. Functionalization of MWCNTs

MWCNTs (3.0 g) were dispersed in 98% concentrated sulphuric acid under ultrasonication at 50°C for 6 h to produce oxidized carbon nanotubes (MWCNT-COOH) [18]. The samples were washed with ultrapure water and dried at 50 °C for 12 h.

2.2. Preparation of MWCNT-COOAg

One gram of MWCNT-COOH was dispersed in 100 mL of distilled water through ultrasonication.

To this solution, 100 mL of 0.2M Ag nitrate solution was added with constant stirring at 60°C to generate Ag ions grafted carbon nanotubes (MWCNT-COOAg). After the completion of reaction, solid products were collected by centrifuging and dried under vacuum at 50°C. Ag ions grafted onto carbon nanotubes were reduced at 200° C to generate Ag nanoparticles on the carbon nanotube surface.

2.3. Antibacterial tests

The antibacterial property of MWCNT-COOH, Ag nanoparticles decorated MWCNTs were evaluated against gram positive *Escherichia coli* (*E. coli*) bacteria [19]. Were used sterile samples with a fix amount of MWCNT-COOAg, MWCNT-COOH and MWCNTs.

Escherichia coli (K 12-MG1655) cultured in a tube containing Luria Bertani medium at 37 ^oC. Luria Bertani medium composition: peptone, 10 g/L; yeast extract 5 g/L, NaCl 5 g/L. These bacteriological experiments performed in vitro demonstrated efficacy of MWCNT-COOAg against growth of *Escherichia coli* bacteria.

Sterile samples were incubated 18 hours of test tubes containing 5 mL culture of *Escherichia coli*. Optical density was determined after 18 hours of incubation. Incubation was performed in the incubator Laboshake Gerhardt.

Optical densities for the three samples and control (*Escherichia coli* culture without sample) were determined by UV-VIS spectrophotometer (Jenway Spectrophotometer).

3. Results

3.1. TEM analysys

The preparation of MWCNT-COOAg involves the introduction on the MWCNTs of acid groups through sulfuric acid treatment, the introduction of Ag ions and the development of Ag nanoparticles.

Acid treatment removes the impurities as amorphous carbon particles and also introduces the –COOH groups on the surface of MWCNTs.

The formation of Ag nanoparticles on the MWCNTs surface is confirmed by TEM (transmission electron microscopy) results.

TEM analysis shows in Fig. 1 the silver nanoparticles with average diameter around 12-18 nm, while MWCNTs having 20-40 nm in diameter, formed from Ag ions grafted onto carbon nanotubes that were reduced at 200° C.

Regarding distribution of silver nanoparticles ImageJ soft were used. Particle size of Ag solutions were determined and the average diameter is between 11.8-17.9 nm.

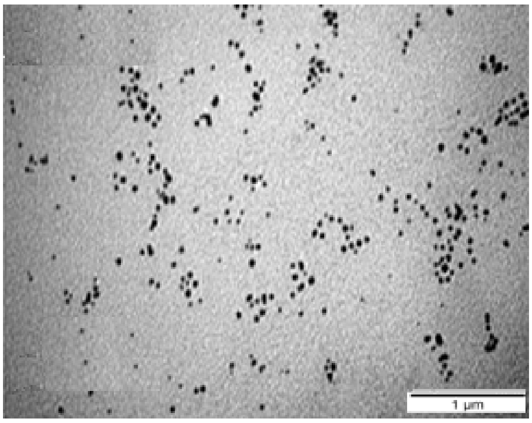

Fig. 1. The TEM images for Ag nanoparticles.

Fig. 2 and Fig. 3 represent the TEM images for MWCNTs nonfunctionalized and functionalized with –COOH, and Fig. 4 the TEM images for MWCNT-COOAg.

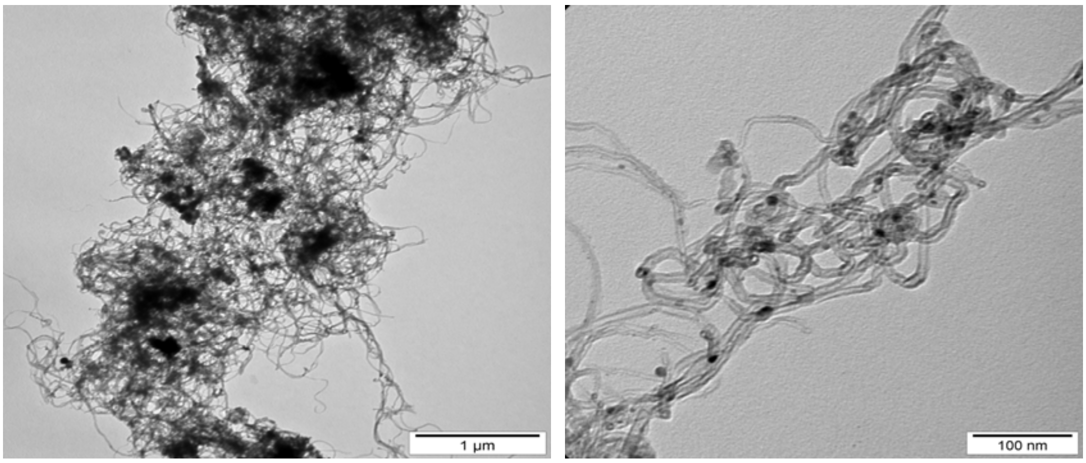

Fig. 2. The TEM images for MWCNTs

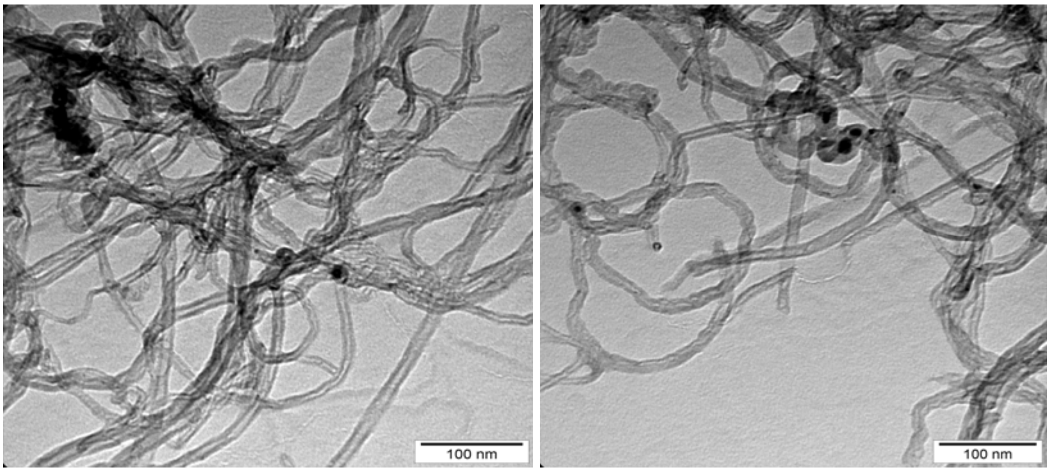

Fig. 3. The TEM images for MWCNT-COOH.

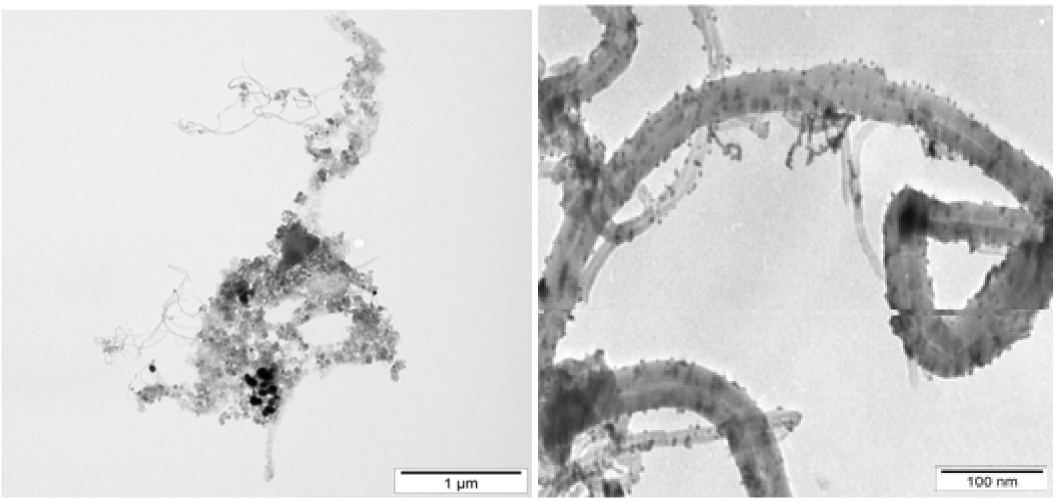

Fig. 4. The TEM images for MWCNT-COOAg.

The attachment of silver nanoparticles on MWCNTs is confirmed by the TEM image. Fig. 4 shows the TEM image of the MWCNTs modifed with silver particles. It can be seen that the silver particles preferentially adhere to the surfaces of MWCNTs rather than to other regions without MWCNTs.

Dark spots corresponds to Ag nanoparticles and light tubes corresponds to MWNTs. The side walls of MWCNTs are evenly decorated with Ag nanoparticles. The density of attached nanocrystals are high. Observed silver particles appear to have a narrow size distribution, and no free particles are observed in the background of the TEM images, which confirms all formed Ag nanoparticles are durably attached to the nanotubes. The size of Ag nanoparticles are significantly smaller than diameter of carbon nanotubes and could be estimated about a few up to a few dozen nm.

3.2. Infrared spectroscopy (FTIR)

FTIR has been used to map the topographic distribution of carbon nanotubes MWCNTs and acid treated MWCNT-COOH. Infrared Microscopy Spectral data were recorded by a Perkin-Elmer equipment.

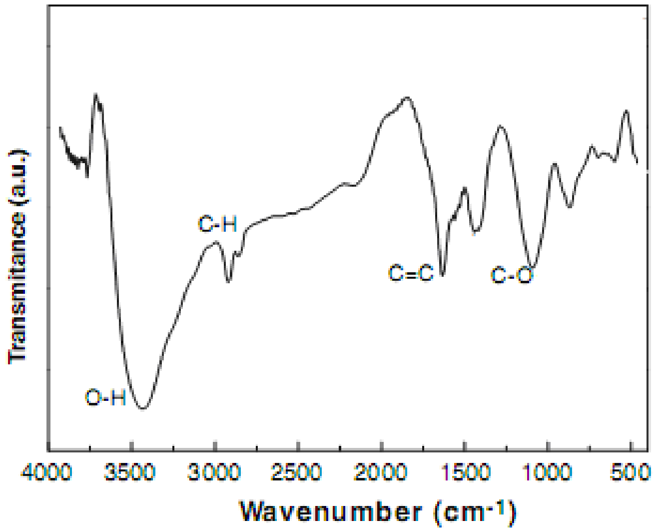

Fig. 5. FTIR spectra of MWCNTs

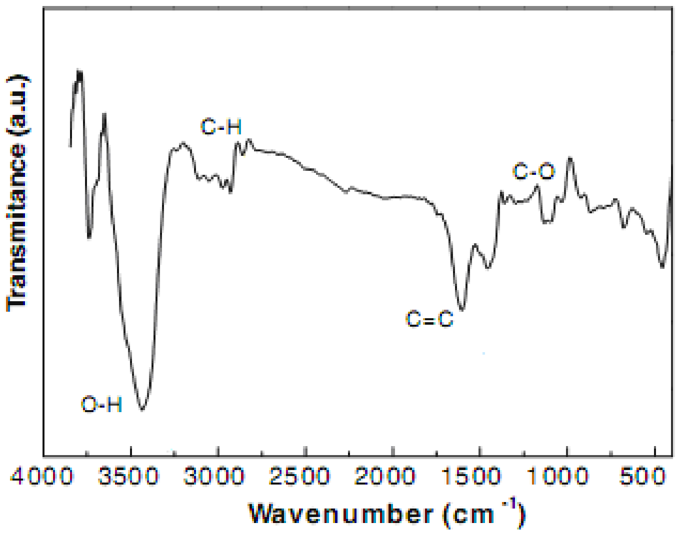

Fig. 6. FTIR spectra of acid-treated MWCNTs.

FTIR spectra from the MWCNTs show a broad peak at 3436 cm^{-1}, which refers to the O-H stretch of the hydroxyl group (Fig. 5), which can be ascribed to the oscillation of carboxyl groups. Carboxyl groups on the surfaces of as-received MWCNTs could be due to the partial oxidation of the surfaces of MWCNTs during purification by the manufacturer. This feature moves to 1726 cm^{-1} and is associated with the stretch mode of carboxylic groups as observed in the IR spectrum of the acid-treated MWCNTs (Fig. 6) [20] indicating that carboxylic groups are formed due to the oxidation of some carbon atoms on the surfaces of the MWCNTs by sulphuric acid. The IR spectra of oxidized MWCNTs shows four major peaks, located at 3750, 3450, 2370, and 1562 cm^{-1}. The peak at 3750 cm^{-1} is attributed to free hydroxyl groups [21]. The peak at 3436 cm^{-1} can be assigned to the O-H stretch from carboxyl groups (O=C−OH and C−OH), while the peak at 2364 cm^{-1} can be associated with the O−H stretch from strongly hydrogen-bonded −COOH. The peak at 1565 cm^{-1} is related to the carboxylate anion stretch mode. The peak at 1631 cm^{-1} can be associated with the stretching of the carbon nanotube backbone. The peaks at around 2877 and 2933 cm^{-1} correspond to the H−C stretch modes of H−C=O in the carboxyl group.

3.3. Antimicrobial test with carbon nanotube solution

MWCNT-COOAg, MWCNT-COOH or MWCNTs antibacterial activities were determined by calculating the percentage inhibition of growth using the formula [17]:

$$I\ \% = [(B_{18} - B_0) - (C_{18} - C_0)]/\ (B_{18} - B_0) \cdot 100$$

where I is the percentage inhibition of growth, B_{18} is the blank- compensated optical density at 600 nm (OD_{600} = 15.8) of the positive control of the organism at 18 h, B_0 is the blank-compensated OD_{600} of the positive control of the organism at 0 h (OD_{600} = 0.078), C_{18} is the negative control-compensated OD_{600} of the organism in the presence of test sample at18 h (OD_{600} = 12.8 (MWCNTs), OD_{600} = 10.5 (MWCNT-COOH), OD_{600} = 5.2 (MWCNT-COOAg)), and C_0 is the negative control-compensated OD_{600} of the organism in the presence of test sample at 0 h (OD_{600} = 0.089).

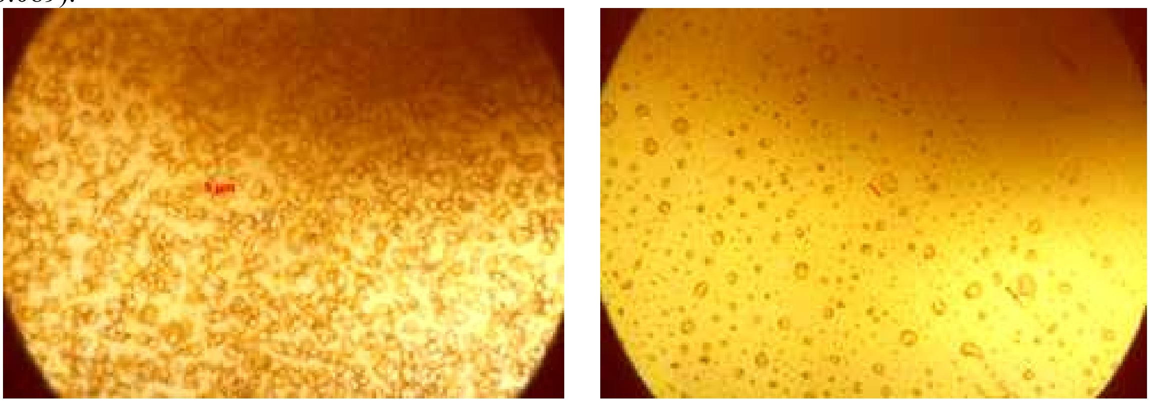

Fig. 7. E. Coli: a. as control b. in MWCNTs

For *E. coli* in MWCNT the inhibition percentage of growth I % = **19 %**

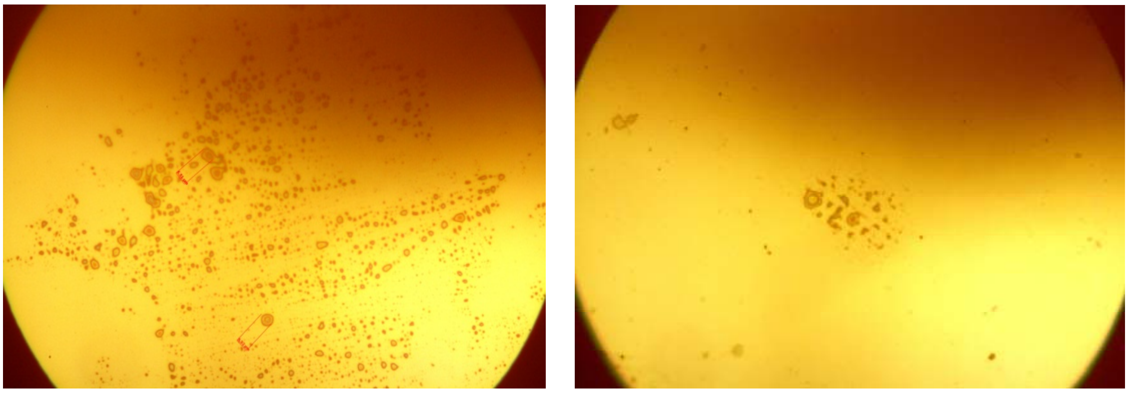

Fig. 8. E. Coli in: a. MWCNT-COOH b. MWCNT-COOAg.

For *E. coli* in MWCNT-COOH is determined the percentage inhibition of growth I % = **34 %** and for E. Coli in MWCNT-COOAg the inhibition is I %= **68 %**

4. Discussion

TEM images on the surface of MWCNTs become rough after the functionalization of MWCNTs with –COOH groups. The average particles sized of the Ag nanoparticles are observed to be between 11.8-17.9 nm. The silver nanopaticles were radial disposed to the intersection of two MWCNTs and in the areas with more agglomerations of nanotubes.

Fig. 9 shows the average optical density of five experiments conducted by the above description:

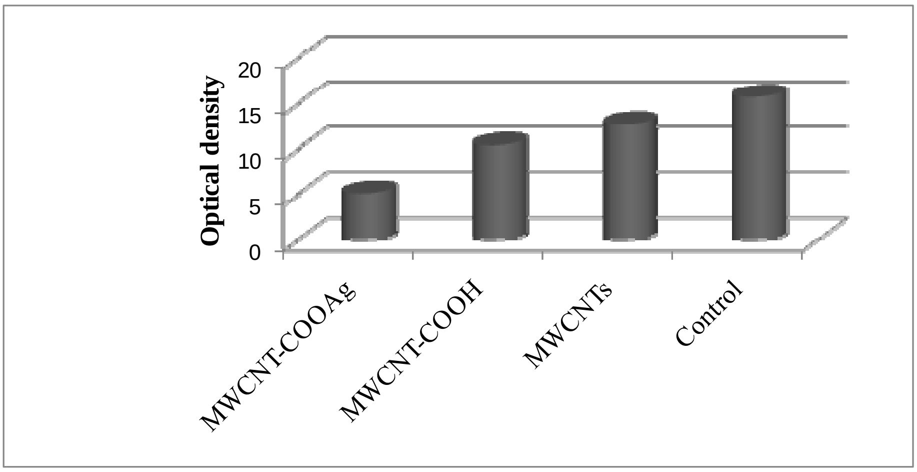

Fig. 9. The average optical density of five experiments for control and three samples.

5. Conclusions

The functionalization of carbon nanotubes induces an increase of the percentage inhibition of *Escherichia coli* bacteria growth from 19% to 34%. A better efficiency in antibacterial effect induces the silver nanoparticles anchorage to the surface of functionalized MWCNTs nanotubes, when the increase of percentage inhibition of bacteria varied from 34% to 68%.

Silver nanoparticles were anchored to the surfaces of MWCNTs nanotubes by a simple electrostatic adsorption and these findings may suggest that MWCNT-COOAg can be used as effective antimicrobial materials that find applications in antibacterial controlling systems.

Acknowledgements

Authors recognise financial support from the European Social Fund through POSDRU/89/1.5/S/54785 project: "Postdoctoral Program for Advanced Research in the field of nanomaterials.

References

[1] X. Wang, Q Li, J. Xie, Z. Jin, J. Wang, Y. Li, K. Jiang, S. Fan, Nano Lett. **9** (9), 3137 (2009).
[2] C. Dekker, Carbon nanotubes as molecular quantum wires, Physics Today **52**, 22 (2009).
[3] Y. Chen, D. Ciuparu, G. L. Haller , S.Lim , L. D. Pfefferle, Carbon **44** (1), 67 (2006).
[4] S.V. Mahajan, S.A. Hasan, J. Cho, M.S.P. Shaffer, A.R. Boccaccini, J. H. Dickerson, Nanotechnology **19,** 195301 (2008).
[5] B.J.C. Thomas, M.S.P. Shaffer, A.R. Boccaccini, J. Am. Ceram. Soc. **88** (4), 980 (2005).
[6] R. Ormsby, T. McNally, C. Mitchell, N. Dunne, J. Mater. Sci Mater. Med. **21**(8), 2287 (2010).
[7] K.K. Chew, K.L. Low, S.H. Sharif Zein, D.S. McPhail, L.C. Gerhardt, J.A.Roether, A.R. Boccaccini, J. Mech. Behav. Biomed. Mater. **4** (3), 331 (2011).
[8] M. Mîndroiu, C. Pirvu, R. Ion, I. Demetrescu, Electrochim. Acta **56** (10), 193 (2010).
[9] I. Demetrescu, C. Pirvu, V. Mitran, Bioelectrochemistry **79**, 122 (2010).
[10] J. Chłopek, B. Czajkowska, B. Szaraniec, E. Frackowiak, K. Szostak and F. Béguin, Carbon **44** (6), 1106 (2006).
[11] J. Kolosnjaj, H. Szwarc, F. Moussa, Adv. Exp. Med. Biol. **620**, 181 (2007).

[12] F. Watari, NanoBiomedicine **1**, 2 (2009).
[13] A. Porter, M. Gass, M. Mhairi, S. Karin, N. Jeremy, P. A. Midgley, M. Welland, Nature Nanotechnology **2** (11), 713 (2007).
[14] N. Lkhgvajav, I. Yasa, E. Celik, M. Koizhaganova, O. Sari, Digest J. Nanomat. Biostruct. **6** (1), 149 (2011).
[15] M. Popescu, A. Velea, A. Lörinczi, Digest J. Nanomat. Biostruct. **5** (4), 1035 (2010).
[16] M. Samim, F. J. Ahmed, M. Z. Abdin, S. Naqzi, Digest J. Nanomat. Biostruct., to be published (2011).
[17] A. Hirsch, O. Vostrowsky, Topics in Current Chemistry **245**, 193 (2005).
[18] S. Jaiswal, B. Duffy, A.K. Jaiswal, N. Stobie, P. Mc Hale, Int. J. Antimicrob., **36** (3), 280 (2010).
[19] R. Mohan, A. M. Shanmugharaj, R. S. Hun, Biomed. Mater. Res. B. Appl. Biomater. **96** (1), 119 (2011).
[20] K. R. Reddy, B. C. Sin, K. S. Ryu, J.-C. Kim, H. Chung, and Y. Lee, Synth. Met. **159**, 595 (2009).
[21] S. Goyanes, G. R. Rubiolo, A. Salazar, A. Jimeno, M. A. Corcuera, I. Mondragon, Diamond Relat. Mater. **16**, 412 (2007).